



저작자표시-비영리-변경금지 2.0 대한민국

이용자는 아래의 조건을 따르는 경우에 한하여 자유롭게

- 이 저작물을 복제, 배포, 전송, 전시, 공연 및 방송할 수 있습니다.

다음과 같은 조건을 따라야 합니다:



저작자표시. 귀하는 원저작자를 표시하여야 합니다.



비영리. 귀하는 이 저작물을 영리 목적으로 이용할 수 없습니다.



변경금지. 귀하는 이 저작물을 개작, 변형 또는 가공할 수 없습니다.

- 귀하는, 이 저작물의 재이용이나 배포의 경우, 이 저작물에 적용된 이용허락조건을 명확하게 나타내어야 합니다.
- 저작권자로부터 별도의 허가를 받으면 이러한 조건들은 적용되지 않습니다.

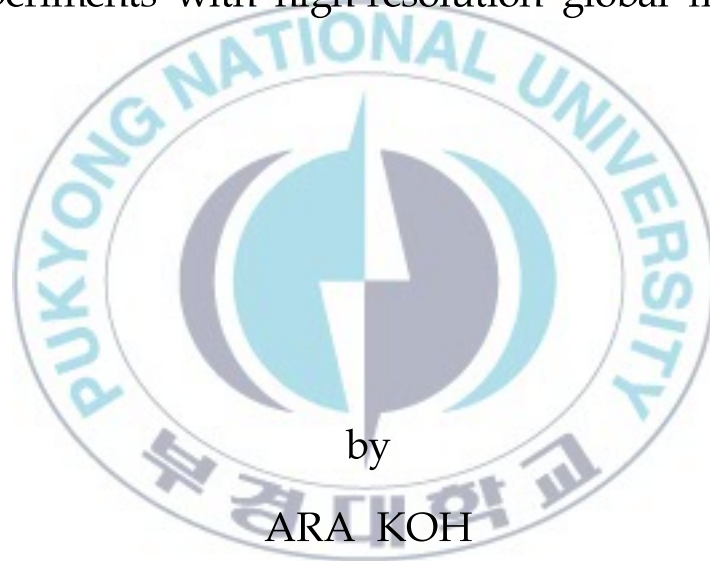
저작권법에 따른 이용자의 권리는 위의 내용에 의하여 영향을 받지 않습니다.

이것은 [이용허락규약\(Legal Code\)](#)을 이해하기 쉽게 요약한 것입니다.

[Disclaimer](#)

Thesis for the Degree of Master of Science

Projections of Tropical Cyclones in a warming world:  
Experiments with high-resolution global model



by

ARA KOH

Department of Environmental Atmospheric Science

The Graduate School

Pukyong National University

August 2010

Projections of Tropical Cyclones in a warming world:  
Experiments with high-resolution global model  
(온난화 시나리오에 따른 미래 태풍 변화에 관한 연구)

Advisor: Prof. Jai-ho Oh

by

ARA KOH



A thesis submitted in partial fulfillment of the requirements  
for the degree of  
Master of Science

in Department of Environmental Atmospheric Science,  
The Graduate School,  
Pukyong National University

August 2010

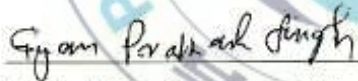
Projections of Tropical Cyclones in a warming world:  
Experiments with high-resolution global model

A dissertation  
by  
ARA KOH

Approved by:



(Chairman) Prof. Hyeong-Bin Cheong



(Member) Prof. Gyan Prakash Singh



(Member) Prof. Jai-Ho Oh

August 25, 2010

# Contents

<b>List of Figures</b> .....	ii
<b>List of Tables</b> .....	iv
<b>Abstract</b> .....	1
<b>I . Introduction</b> .....	3
<b>II . Methodology</b> .....	6
1. Model and experiment .....	6
2. Tropical cyclone identification method .....	19
3. Validation of GME output with observation .....	21
<b>III . Results</b> .....	25
1. Results of high-resolution time-slice experiments .....	25
2. An example of a tropical cyclone .....	29
3. Tracks and geographical distribution .....	33
4. Frequency, Duration, and Intensity in West Pacific region .....	35
<b>IV . Summary and Conclusions</b> .....	40
<b>References</b> .....	42

## List of Figures

- Fig. 1** Grid generation by successively halving the triangle edges to from new triangles. Parameter  $n_i$  is the number of intervals on a major triangle edge. .... 8
- Fig. 2** Schematic diagram of the sea surface temperature (SST) setting used for the middle of the 21st century and end of 21st century simulation under IPCC-AR4 A1B scenario. .... 16
- Fig. 3** Performance process of the GME. .... 18
- Fig. 4** Tropical Cyclone Centers and their regions image courtesy of the World Meteorological Organization. .... 21
- Fig. 5a-f** (a) Mean temperature of five years at 2m for presents day climate experiment, (b) difference between Middle of 21st century and present experiments and (c) difference between End of 21st century and present experiments in DJF (left panel) and JJA (right panel) seasons. .... 26
- Fig. 6a-f** Same as in Fig. 5 (a-f) except for precipitation. .... 28
- Fig. 7** A typhoon simulated with the 40 km GME global model. (a) A week tropical storm was generated of the simulation at 14°N, 162°E. (b) The tropical strom moved westward and developed slowly. (c) It developed tropical cyclone over 23 m/s and turned its direction to north-westward. (d) The simulated typhoon wind speed over 42 m/s. .... 30

**Fig. 8** Horizontal view of a tropical cyclone simulated in the present-day experiment (Nov 1, 2nd year of the time integration): horizontal distributions of (a) PMSL (line) and wind speed at 850 hPa (shaded) in the northwest Pacific region, (b) daily averaged precipitation amount in mm hour<sup>-1</sup> (shaded), (c) relative vorticity (shaded), (d) difference of wind speed at 850 hPa and 300 hPa (shaded), (e)(f) difference of temperature at 700 hPa and 500 hPa (shaded), and 700 hPa and 300 hPa (shaded). ..... 32



## List of Tables

<b>Table 1</b>	Summary of models used in tropical cyclone study .....	5
<b>Table 2</b>	Some characteristic quantities of the icosahedral-hexagonal grid at different resolutions given by $n_i$ , the number of intervals on a main triangle side. $N=10n_i^2+2$ is the number of grid points, $A_{\min}$ is the minimum grid cell area, $A_{\max}$ is the maximum grid cell area. $\Delta_{av}$ is the mean, $\Delta_{\min}$ the minimum, and $\Delta_{\max}$ the maximum distance between grid points. ....	11
<b>Table 2.a</b>	The main triangle side is halved $q$ times, i.e. $n_i=2^q$ , where $q$ is a positive integer. ....	11
<b>Table 2.b</b>	The main triangle side is first divided into three intervals, after that halved $l$ times, i.e. $n_i=3*2^l=2^q$ , $q=1.585+l$ . ....	11
<b>Table 3</b>	Summary of Physical parameterization methods in GME ....	12
<b>Table 4</b>	The Emissions Scenarios of the Special Report on Emissions Scenarios (SRES) (IPCC, 2001) .....	14
<b>Table 5</b>	Projected global average $CO_2$ concentration, temperature and sea level rise at the end of the 21 <sup>st</sup> century. ....	15
<b>Table 6</b>	Setup for 40 km Time-slice experiments .....	17
<b>Table 7</b>	A list of the Regional Specialized Meteorology Centers (RSMC) and Tropical Cyclone Warning Centers (TCWC) participating in the WMO Tropical Cyclone Programme. ....	22
<b>Table 8</b>	Tropical Cyclone region in this paper. ....	23

## 미래 태풍에 관한 전망

### 고 아 라

부 경 대 학 교   대 학 원   환 경 대 기 과 학 과

#### 요 약

기후시스템은 여러 가지 자연적 요인(태양변화, 화산폭발로 인한 성층권의 에어로솔의 변화, 천문학적 요인 등)과 인위적 요인(온실 기체의 배출, 산림의 파괴, 도시화 등)에 의해 과거와 다른 양상을 보이며 계속적으로 변화하고 있다. 2007년 발간된 유엔정부간 기후변화위원회(International Panel in Climate Change, IPCC) 제4차 보고서(2007)에서 지구온난화는 논란의 여지가 없을 정도로 명백하다고 평가하고 있다. 1906년 이후 100년간 전지구 평균기온이 0.74° C 증가하였으며 최근 12년(1995~2006)년 중 11년이 최고기록을 가진다고 보고되었다. 특히 전구평균 해수면의 상승과 북극해빙면적의 감소 등이 지구온난화의 증거로 제시되었으며, 다양한 온실가스 배출시나리오에 의한 결과로부터 21세기는 20세기 기후변화보다 클 가능성이 매우 높고 2100년 지구평균기온변화는 1.1~6.4° C로 온실가스 배출량에 비례할 것으로 전망하였다. 이러한 기후변화는 자연재해에도 영향을 미친다. Tropical cyclone은 인류가 겪는 자연재해 중 인명과 재산에 가장 큰 피해를 주는 것 중 하나로 기후변화에 따른 미래 변화가 과학적 관점과 사회·경제적 관점에서 우선적인 이슈가 되고 있다.

Tropical cyclone의 미래 변화 양상을 보기 위해 수행되어야 할 미래 기후변화 예측에 관한 연구는 전구 규모의 순환을 연구하기 위해 개발된 대기 대순환 모델(Atmospheric General Circulation Model, AGCM)이 전통적인 방법으로 사용되고 있다. 하지만 지금까지 이루어진 대부분의 연구에서는 시공간 분해능의 한계로 인해 상세한 지역적인 정보를 제공해주지 못하였고, 이를 해결한 고해상도의 AGCM 자료는 일부에서 이루어지고 있다. 따라서 본 연구에서는

Tropical cyclone 분석을 위한 세밀한 규모의 미래 기후 정보를 얻기 위해 진보된 격자체계인 Icosahedral-hexagonal grid-point를 가진 GME 모델을 이용한다. 모델의 초기자료는 ECMWF MARS (European Centre for Medium-Range Weather Forecasts Meteorological Archive and Retrieval System)의 operating analysis data를 사용하고, IPCC A1B emission scenario(IPCC 2001)에 따른 100 km 이상의 해상도를 가진 4개 모델 수행 결과에서 얻어진 평균 SST와 Sea-ice를 forcing으로 사용한다. 수평해상도 40 km로 현재(1979~1983), 21세기 중반(2041~2045), 21세기 후반(2081~2085)의 각각 5년의 기간을 Time-slice 기법으로 모의하여 고해상도 시나리오 자료를 분석한다.

모의 결과 서태평양 지역에 발생하는 태풍에 대해, 관측과 현재 모의는 태풍 분포가 유사하게 나타났고, 태풍의 특성을 잘 나타내었다. 이를 바탕으로 현재 모의와 21세기 중반, 후반의 모의를 비교한 결과 빈도수가 미래로 갈수록 감소하는 추세를 나타내었고, 강도는 점차 증가하는 추세를 보였다. 또한 태풍 생존 기간 분석에서는 현재보다 미래에 주기가 줄어드는 경향을 보였으나, 21세기 중반과 후반을 비교하였을 때, 중반보다 후반이 0.2일 정도 길 것으로 예상된다.

본 결과는 단순한 변동을 넘어서 인류에게 심각한 영향을 미치고 있는 Tropical cyclone을 예측함으로써, 미래 사회경제적 영향을 최소화 시킬 수 있는 하나의 정보가 될 것이다.

**주요어:** 기후 변화, AGCM, SRES A1B 시나리오, Tropical Cyclone, 태풍

# I . Introduction

Tropical cyclones (TC) are most devastating natural disasters because of loss of human life they cause and the large economics losses they induce. Vulnerability to TC is becoming more pronounced because of rapid growth in populations near the tropical coastal zones. A TC is a non frontal synoptic scale low pressure system originating over the tropical or subtropical oceans. TC with maximum surface wind speed of less than 17m/s are generally known as tropical depression. Once a TC achieved surface wind strength of 17m/s, it is typically known as tropical storm or tropical cyclone. If the surface wind speed reach 33m/s, the tropical storm is known as typhoon (over the North West Pacific Ocean); or a severe tropical cyclone (over the South Pacific and Indian Oceans); or Hurricane (over North Atlantic and Northeast Pacific Oceans). Simulation of TC is a challenging problem among the scientists to fully understand the genesis, development and decaying characteristics of TCs. Recently, many modeller are attempting to associate TCs trend with climate change caused by greenhouse warming.

Warming of the earth climate system is unequivocal as it is now. There are several evidences based on observations and modelling

studies which show an increase in global average surface air and ocean temperatures, widespread melting of snow and ice, and global sea level rising (IPCC, 2007).

Due to increase in surface air temperature, a variety of climate change phenomena can be observed. One of the devastating phenomenon is tropical cyclone. Globally, the estimates of the potential destructiveness by Tropical cyclone shows a significant increasing trends since the mid 1970's, trend of longer lifetimes of TC and greater storm Intensity and such trends may be strongly correlated with the tropical ocean SST.

Intense hurricane, wind speed of above 114 knots occur frequently due to increase in global temperature during 1990 to 2004 (Webster et al., 2005). Simulation of tropical cyclones over the Northwest Pacific sector under CO<sub>2</sub>-warmed environments (CO<sub>2</sub> increases at 1%/year) using high-resolution regional model indicate a increase in frequency of tropical cyclone (Knutson et al., 1998). Further, it is found that a maximum wind speeds of hurricanes will strengthen up to 3~10% during next 100 years (Knutson et al., 2001).

The above inferences are based on observational and simulation studies through regional models. However, Oouchi et al. (2006) has projected a significant decrease in the frequency of tropical cyclone by 30 %, but a significant increase in the intensity under the greenhouse-warmed environments. There are several groups using

different models and resolution under different CO<sub>2</sub> emission scenarios to understand characteristics of TC associated with global warming environment. The summary of models are given in Table 1.

An attempt has been made to study the influence of global warming on tropical cyclones globally using Global Atmospheric model GME in Time-slice experiments.

**Table 1** Summary of models used in tropical cyclone study

Reference	Model	Resolution	Scenario
Sugi et al.(2002)	JMA GSM8911	T106	CO <sub>2</sub> ×2
Tsutsui (2002)	NCAR CCM2	T42	CO <sub>2</sub> ×2
Hasegawa and Emori (2005)	CCRS/NIES/ FRCGC	T106	CO <sub>2</sub> ×2
Yoshimura and Sugi (2005)	JMA GSM8911	T106	CO <sub>2</sub> ×2 CO <sub>4</sub> ×2
Oouchi et al. (2006)	MRI/JMA	20 km	A1B
Yoshimura et al. (2006)	JMA GSM9603 (Arakawa-Schubert)	T106	CO <sub>2</sub> ×2
Bengtsson et al. (2007)	ECHAM5	T63 T213 T319	A1B

## II . Methodology

### 1. Model and experiment

#### 1.1 Model description

GME, a hydrostatic model, has basically a new operational global weather forecast model developed by Deutscher Wetterdienst (DWD), employs a grid-point approach with an almost uniform Icosahedral-hexagonal grid. GME replaced GM(the operational global model derived from the spectral model of the European Centre for Medium Range Weather Forecast) and EM(regional model for central Europe) (Majewski et al., 2002). Descriptions of the design and implementation of the geodesic model GME, including shallow water tests and an evaluation of the dynamical core of the model, are well described in Majewski (1998).

Using a high-resolution atmospheric general circulation, GME has several advantages: a major advantage of the icosahedral-hexagonal grid is the avoidance of the so-called pole problem that exists in conventional latitude-longitude grids. The

singularities at the poles lead to a variety of numerical difficulties including a severe limitation on the time step, size unless special measures are undertaken. It is more competitive at higher resolution than at lower resolution (Ringler et al., 2000). Tomita and Satoh (2004b) have shown that the grid point method using a quasi-uniform grid system (e.g. Nonhydrostatic Icosahedral Atmospheric Model) has computational advantages over the spectral model at higher resolution (scale of which corresponds to 40 km). The grid point approach also avoids the large amount of global communication required by spectral transform techniques. The dynamical core incorporates many of the positive features of spectral models and finite-difference models into a single framework.



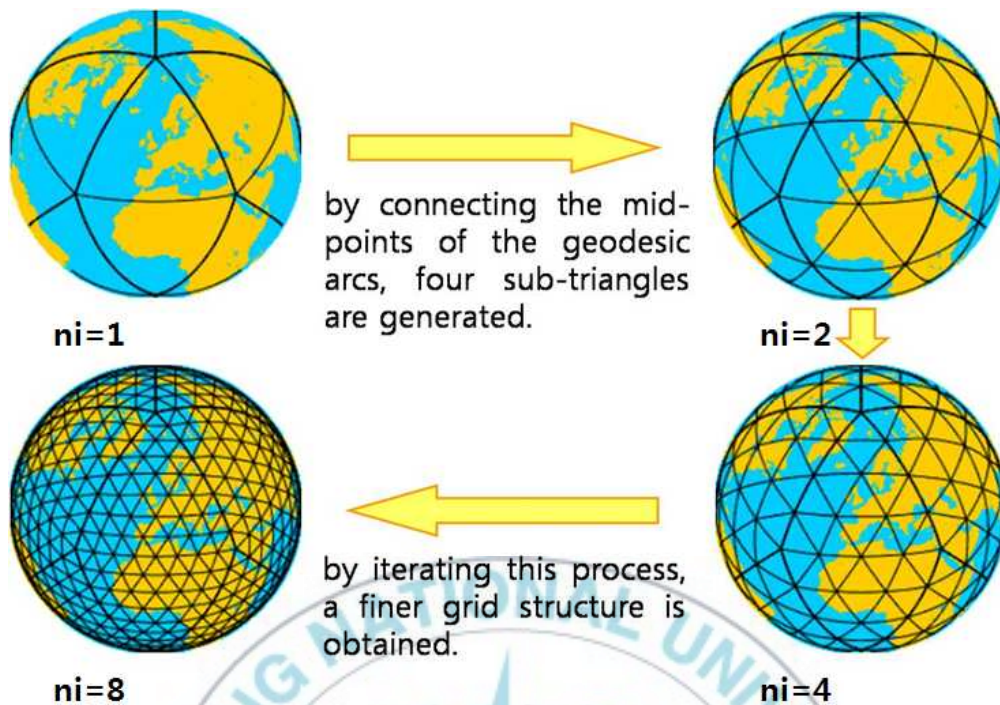


**Fig.2** Grid generation by successively halving the triangle edges to form new triangles. Parameter  $n_i$  is the number of intervals on a major triangle edge.

Regular Icosahedron is constructed inside the sphere in such a way that out of its 12 vertices, 2 vertices are coincided with the North and South Poles. Beginning from this grid of Icosahedral triangles, a new finer grid of triangles are generated by connecting mid points of the spherical triangle sides by an additional set of great circle arcs. This process may be repeated until a grid of the desired resolution is obtained (shown in Fig.1).

The spacing of the icosahedral-hexagonal grid of the GME is determined by the parameter  $n_i$  which is the number of intervals on a main triangle side (of a length of about 7,054 km). Table 2 gives an overview of the grid characteristics for different values of  $n_i$ .

The vertical discretization of GME is based on a hybrid coordination system (sigma-pressure) after *Simmons and Burridge (1981)*. The pressure  $p_h$  at the layer interfaces (=half levels) is given by:

$$p_h(j1,j2,j3,jd) = a_k(j3) + b_k(j3) * ps(j1,j2,jd)$$

where  $a_k$  and  $b_k$  represent vertical co-ordinate parameters,

with  $j3 = 1, i3e+1$  where  $i3e$  is the number of GME layers. ( $i3e=40$ ),

$ps$  time-dependent surface pressure on the orography of the model,

$j1 = 0, n_i$  row index,

$j2 = 1, n_i+1$  column index,

$jd = 1, 10$  diamond index.

The pressure  $p_f$  at the center of the layer (full levels), where

most variables of the GME are defined, is given by the arithmetic mean of the pressure values at the adjacent half levels:

$$p_f(j_1, j_2, j_3, j_d) = 0.5 * (p_h(j_1, j_2, j_3, j_d) + p_h(j_1, j_2, j_3 + 1, j_d))$$

with  $j_3 = 1, i_3e$ .

In this study,  $n_i=192$ , i.e. the mean grid spacing of GME is 40 km, and the mean grid cell is  $1,384 \text{ km}^2$ . The lowest full level is about 10 m above the model orography, and the uppermost full level is placed at 10 hPa.

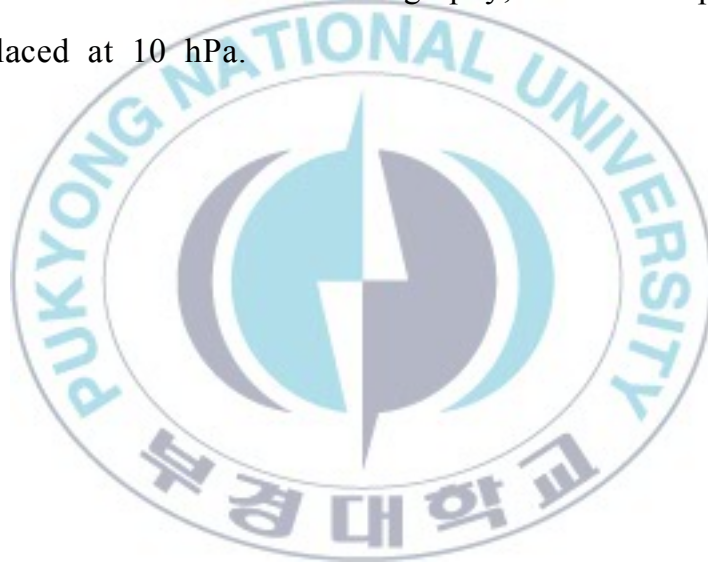


**Table 2** Some characteristic quantities of the icosahedral-hexagonal grid at different resolutions given by  $n_i$ , the number of intervals on a main triangle side.  $N=10n_i^2+2$  is the number of grid points,  $A_{\min}$  is the minimum grid cell area,  $A_{\max}$  is the maximum grid cell area.  $\Delta_{av}$  is the mean,  $\Delta_{\min}$  the minimum, and  $\Delta_{\max}$  the maximum distance between grid points.

**Table 2.a** The main triangle side is halved  $q$  times, i.e.  $n_i=2^q$ , where  $q$  is a positive integer.

q	$n_i$	N	$A_{\min}$ ( $\text{km}^2$ )	$A_{\max}$ ( $\text{km}^2$ )	$\Delta_{av}$ (km)	$\Delta_{\min}$ (km)	$\Delta_{\max}$ (km)
4	16	2562	154109	238061	477.6	440.5	526.0
5	32	10242	38515	59955	239.3	220.3	263.2
6	64	40962	9628	15017	119.8	110.1	131.6
7	128	16842	2407	3756	59.9	55.1	65.8
8	256	655362	602	939	30.0	27.6	32.9
9	512	2621442	150	235	15.0	13.8	16.5

**Table 2.b** The main triangle side is first divided into three intervals, after that halved  $l$  times, i.e.  $n_i=3 \cdot 2^l=2^q$ ,  $q=1.585+l$ .

q	$n_i$	N	$A_{\min}$ ( $\text{km}^2$ )	$A_{\max}$ ( $\text{km}^2$ )	$\Delta_{av}$ (km)	$\Delta_{\min}$ (km)	$\Delta_{\max}$ (km)
4.6	24	5762	68477	97683	319.0	293.7	346.9
5.6	48	23042	17117	24494	159.7	146.8	173.5
6.6	96	92162	4279	6128	79.7	73.4	86.8
<b>7.6</b>	<b>192</b>	<b>368642</b>	<b>1070</b>	<b>1532</b>	<b>40.0</b>	<b>36.7</b>	<b>43.4</b>
8.6	384	1474562	267	383	20.0	18.4	21.7
9.6	768	5898242	67	96	10.0	9.2	10.9

Geodesic model GME generally employs the same methods and procedures as applied in NWP (Numerical Weather Prediction) grid schemes. Different Physical parameterization methods used in GME are summarized in Table 3.

**Table 3** Summary of Physical parameterization methods in GME

Radiation and clouds	Ritter and Geleyn (1992)
Grid-scale precipitation	Doms and Schattler (2003)
Convection	Tiedtke (1989)
Turbulent fluxes in the ABL and the free atmosphere	Muller (1981), based on Louis (1979) Mellor and Yamada (1974)
Soil model	Heise and Schrodin (2002)
SSO scheme	Lott and Miller (1997)

## 1.2 The time-slice experiments

The major tool used to assess the anticipated climate change caused by increase in concentration of greenhouse gases are simulated with global models (GME). The changes in the concentrations of various greenhouse gases have been prescribed according to typical scenarios provided by the Intergovernmental Panel on Climate Change (IPCC). Table 4 shows the representative emissions scenarios of the Special Report on Emissions Scenarios (SRES) (IPCC, 2001).

To predict future climate, simulation using different Emissions Scenarios are demonstrated in many studies (Oouchi et al. (2006), Sugi et al. (2002)). Among them the A1B scenario represent more balanced condition (where balanced is defined as not relying too heavily on one particular energy source, on the assumption that similar improvement rates will be applied to all energy supply and end-use technologies). Based on A1B emission scenario, it is projected that the CO<sub>2</sub> concentration is likely to be 720 ppm, increase in temperature is likely to be 2.8°C and Sea level rise is likely to be from 0.21 to 0.48 m. The detail about different scenarios and projected concentration of CO<sub>2</sub>, temperature and sea level rise are given in Table 4 and Table 5 respectively.

**Table 4** The Emissions Scenarios of the Special Report on Emissions Scenarios (SRES) (IPCC, 2001)

**A1.** The A1 storyline and scenario family describes a future world of very rapid economic growth, global population that peaks in mid-century and declines thereafter, and the rapid introduction of new and more efficient technologies. Major underlying themes are convergence among regions, capacity building and increased cultural and social interactions, with a substantial reduction in regional differences in per capita income. The A1 scenario family develops into three groups that describe alternative directions of technological change in the energy system. The three A1 groups are distinguished by their technological emphasis: fossil intensive (A1FI), non-fossil energy sources (A1T), or a balance across all sources (A1B) (where balanced is defined as not relying too heavily on one particular energy source, on the assumption that similar improvement rates apply to all energy supply and end-use technologies).

**A2.** The A2 storyline and scenario family describes a very heterogeneous world. The underlying theme is self-reliance and preservation of local identities. Fertility patterns across regions converge very slowly, which results in continuously increasing population. Economic development is primarily regionally oriented and per capita economic growth and technological change more fragmented and slower than other storylines.

**B1.** The B1 storyline and scenario family describes a convergent world with the same global population, that peaks in mid-century and declines thereafter, as in the A1 storyline, but with rapid change in economic structures toward a service and information economy, with reductions in material intensity and the introduction of clean and resource-efficient technologies. The emphasis is on global solutions to economic, social and environmental sustainability, including improved equity, but without additional climate initiatives.

**B2.** The B2 storyline and scenario family describes a world in which the emphasis is on local solutions to economic, social and environmental sustainability. It is a world with continuously increasing global population, at a rate lower than A2, intermediate levels of economic development, and less rapid and more diverse technological change than in the A1 and B1 storylines. While the scenario is also oriented towards environmental protection and social equity, it focuses on local and regional levels.

**Table 5** Projected global average CO<sub>2</sub> concentration, temperature and sea level rise at the end of the 21<sup>st</sup> century.

SRES	CO <sub>2</sub> Concentration	Temperature (°C)	Sea Level (m)
B1 scenario	550 ppm	1.8(1.1 ~ 2.9)	0.18 ~ 0.38
A1T scenario	540 ppm	2.4(1.4 ~ 3.8)	0.20 ~ 0.45
B2 scenario	600 ppm	2.4(1.4 ~ 3.8)	0.20 ~ 0.43
<b>A1B scenario</b>	<b>720 ppm</b>	<b>2.8(1.7 ~ 4.4)</b>	<b>0.21 ~ 0.48</b>
A2 scenario	830 ppm	3.4(2.0 ~ 5.4)	0.23 ~ 0.51
A1FI scenario	970 ppm	4.0(2.4 ~ 6.4)	0.26 ~ 0.59

Present study conducted three time-slice experiments with GME (Global model). Three time-slice experiments are run for the present climate conditions (1979 ~ 2008), middle of 21<sup>st</sup> century climate condition (2041 ~ 2060), and end of 21<sup>st</sup> century climate condition (2081 ~ 2100). Present-day time-slice experiment is forced with the observed AMIP daily SST and SEA-ICE from 1979 to 2008. While the SST boundary conditions for future time-slice experiments are prepared by superimposing, (i) the trend of SST in IPCC AR4 simulation based on A1B scenario and SEA-ICE dataset, (ii) future

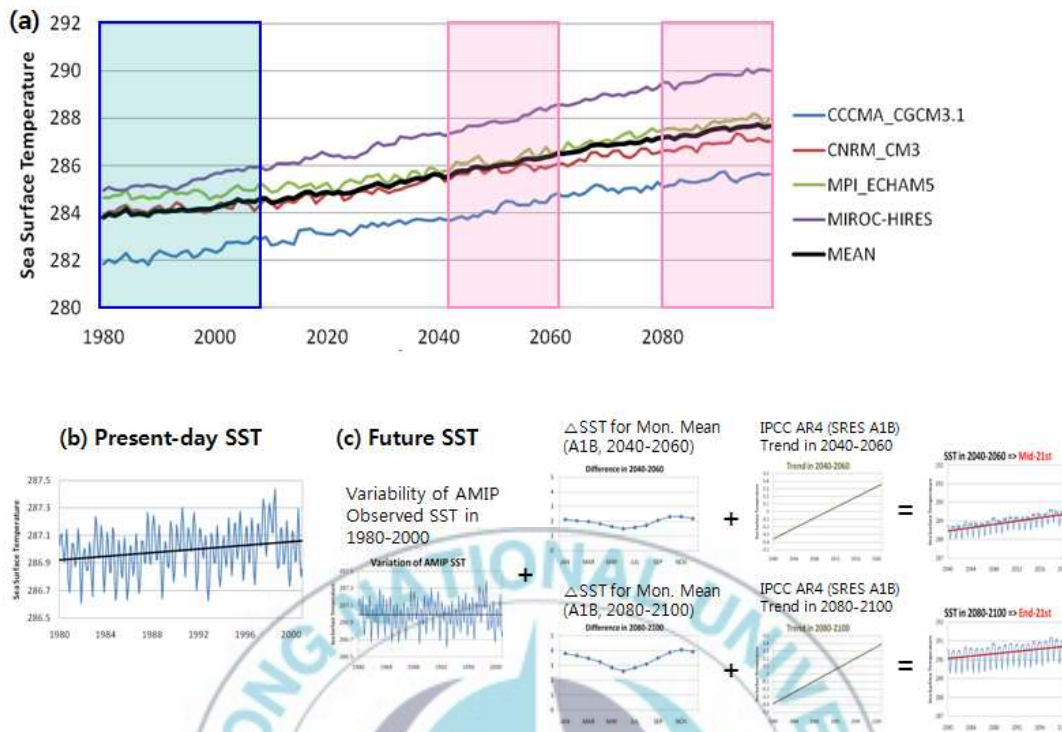


**Fig. 3** Schematic diagram of the sea surface temperature (SST) setting used for the middle of the 21st century and end of 21st century simulation under IPCC-AR4 A1B scenario.

change in SST ( $\Delta$ SST) and (iii) the detrended observed SST anomalies for the period 1979-2008 (Fig. 2).

The three time-slice experiments and SST boundary conditions are described in Table 6. Based on these boundary conditions of SST and SEA-ICE, TCs are simulated with GME using initial data sets. The initial data is the operational data sets provided from the atmospheric model archived of ECMWF, triangular truncation at wave number 511 (T511) and 91 layers. The wave number 511

**Table 6** Setup for 40 km Time-slice experiments

Experiment	Period	Boundary Conditions for SST and SEA-ICE
Time-slice experiment with GME (40 km)	Present-day (1979~2008)	AMIP II Observed SST and SEA-ICE
	Middle of 21C (2041~2060)	GCMs based on SRES A1B averaged SST and SEA-ICE
	End of 21C (2081~2100)	

means 40 km resolution.

All process for the simulating future climate using GME model is as in Figure 3. In pre-processing, change the initial data is made from gaussian grid to icosahedral-hexagonal grid in GME model. Then, simulating the GME model with Multi Layer Soil model during each years, post-processing in the model. It makes the output grid whether model grid (icosahderal-hexagonal grid) or regular-grid. Here, I choose regular-grid to analyze using GrADS program.

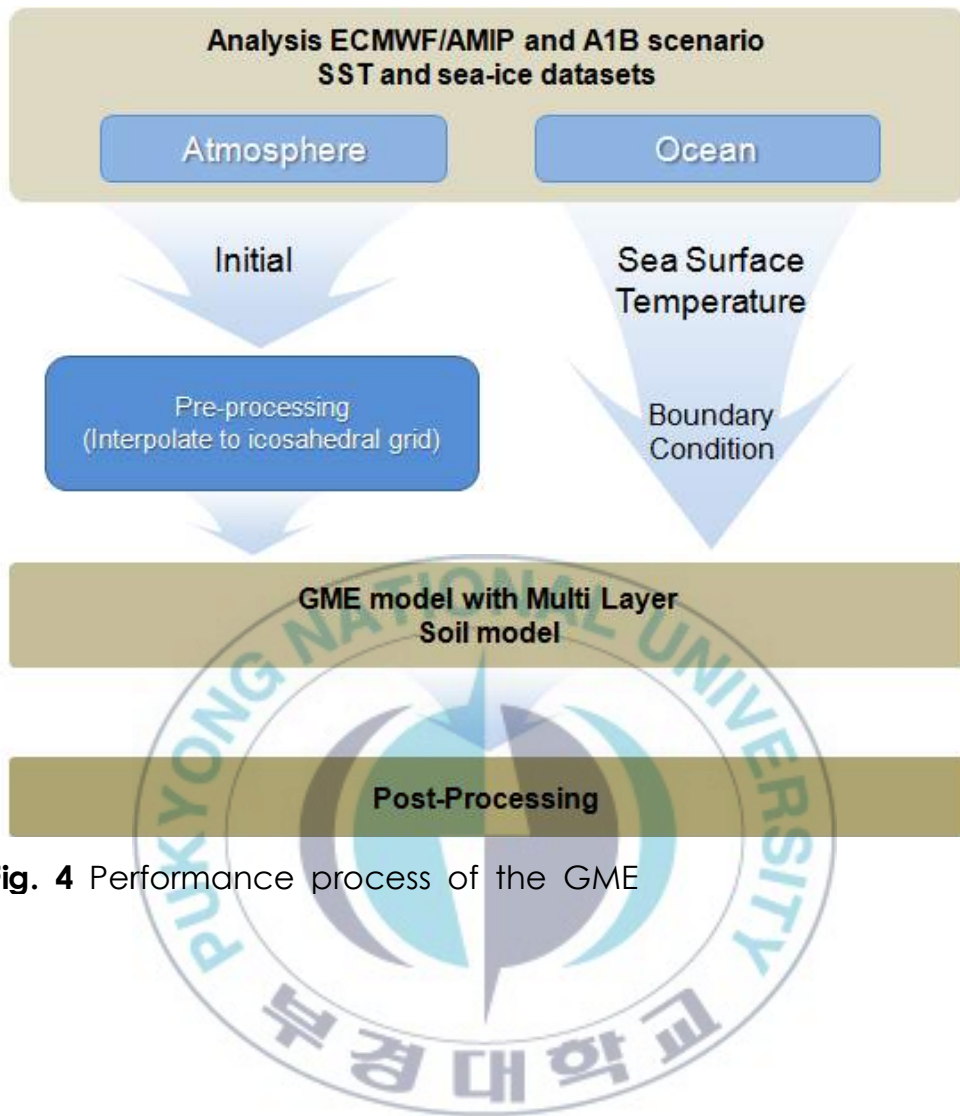


**Fig. 4** Performance process of the GME

## 2. Tropical cyclone identification method

This section focuses on elucidating the difference in tropical cyclone climatology between the present-day climate condition and futures condition, greenhouse-warmed climate condition derived from the 5-year (from 1979 to 1983) time integration period. The difference in the tracks (geographical distributions) and maximum wind speed are mainly studied. The data size of the default, 40 km-mesh output including the basic meteorological elements of the dynamical and thermodynamical physical quantities are about 51 GB per month.

To identify the tropical cyclones from GME simulation for present-day and future experiments, following criteria are used. The target area covers 45 S and 45 N latitudinal belts over the oceans. The initial location of each tropical cyclone was limited in the belt between 30 S and 30 N. Over selected area, the tropical cyclones are identified with the following 6 sets of criteria, which are basically the same as used by Sugi et al. (2002), Oouchi et al. (2006) and originally in line with those of Bengtsson et al. (1996).

- (1) Between 45S~45N latitudinal belt, the grid point corresponding to a TC-center candidate was defined as the one where the minimum surface pressure is at least 2 hPa lower than the

mean surface pressure over the surrounding  $7 \text{ degree} \times 7 \text{ degree}$  grid box.

- (2) The magnitude of the maximum relative vorticity at 850 hPa exceeds  $3.5 \times 10^{-5} \text{ s}^{-1}$ .
- (3) The maximum wind speed at 850 hPa is larger than  $15 \text{ m s}^{-1}$ .
- (4) The temperature structure aloft has a marked warm core such that the sum of the temperature deviations at 300, 500 and 700 hPa exceeds 2 K.
- (5) The maximum wind speed at 850 hPa is larger than wind speed at 300 hPa.
- (6) The duration is not shorter than 48 hours.

Criteria (2)~(6) were applied to the region near the tropical cyclone center to the cases which is satisfying criterion (1).

### 3. Validation of GME output with observation

To verify the simulated tropical cyclone climatology, a global data set for tropical cyclone are obtained from the website;(UNISYS: <http://weather.unisys.com/hurricane>); Combines data for the "best track" tropical cyclone from the National Hurricane Center (NHC) of the U.S. National Oceanic & Atmospheric Administration, and from the U.S. Joint Typhoon Warning Center (JTWC) are used here. The NHC data set contains tracks of tropical cyclones over the North Atlantic and the east North Pacific basins. The JTWC data set

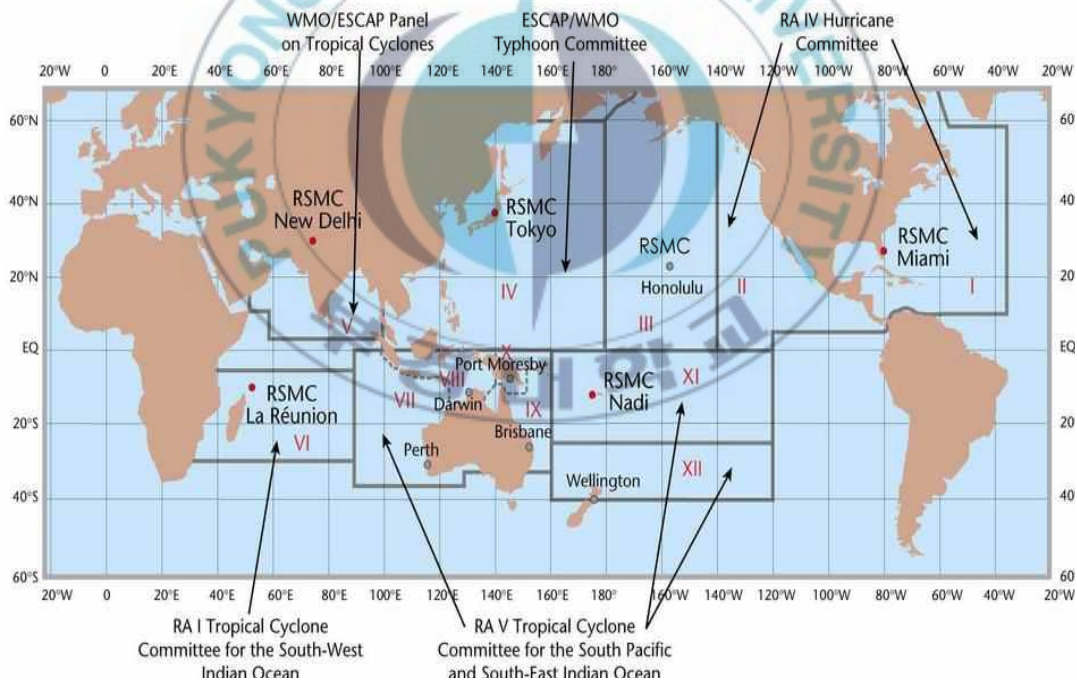


**Fig. 4** Tropical Cyclone Centers and their regions image courtesy of the World Meteorological Organization.

**Table 7** A list of the Regional Specialized Meteorology Centers (RSMC) and Tropical Cyclone Warning Centers (TCWC) participating in the WMO Tropical Cyclone Programme.

Region	Description	Links to Centers (RSMC and TCWC)
<b>I-II</b>	Atlantic and Eastern Pacific	National Hurricane Center (RSMC Miami)
<b>III</b>	Central Pacific	Central Pacific Hurricane Center (RSMC Honolulu)
<b>IV</b>	Northwest Pacific	Japan Meteorological Agency (RSMC Tokyo)
<b>V</b>	North Indian Ocean	India Meteorological Department (RSMC New Delhi)
<b>VI</b>	Southwest Indian Ocean	Météo France (RSMC La Réunion) en Français
<b>VII-X</b>	Southwest Pacific and Southeast Indian Ocean	Australian Bureau of Meteorology (TCWC Perth) Australian Bureau of Meteorology (TCWC Darwin) Papua New Guinea (TCWC Port Moresby) Australian Bureau of Meteorology (TCWC Brisbane)
<b>XI-XII</b>	South Pacific	Fiji Meteorological Service (RSMC Nadi) Meteorological Service of New Zealand, Ltd. (TCWC Wellington)

contains tracks of tropical cyclones over the western North Pacific Ocean, the North Indian Ocean, and the Southern Hemisphere. The region I analyzed based on Figure 4 from National Hurricane Center (<http://www.nhc.noaa.gov/>). The details about sources of data are well described in Table 7. Reanalysis tropical cyclone region are in Table 8.

**Table 8** Tropical Cyclone region in this paper.

Region	Region (by Table 7)	Latitudes	Longitudes
Global	<b>I ~ XII</b>	45S - 45N	ALL
Northern Hemisphere	<b>I ~ V</b>	0 - 45N	ALL
Southern Hemisphere	<b>VI ~ XII</b>	0 - 45S	ALL
North Indian Ocean	<b>V</b>	0 - 45N	30E - 100E
Western North Pacific Ocean	<b>IV</b>	0 - 45N	100E - 180
Eastern North Pacific Ocean	<b>II ~ III</b>	0 - 45N	180 - 90W
North Atlantic Ocean	<b>I</b>	0 - 45N	90W - 0
South Indian Ocean	<b>VI ~ VII</b>	0 - 45S	20E - 135E
South Pacific Ocean	<b>IX ~ XII</b>	0 - 45S	135E - 90W

Out of the datasets, I retrieved only those dataset which have maximum surface wind speed of  $17.2 \text{ m s}^{-1}$  (34 kt) or above, and over 48 hours (2 days) duration from 1979 to 1983 for our analyse.



### III. Results

#### 1. Results of high-resolution time-slice experiments

Present study mainly focuses on temperature at 2m (2m represent better information of temperature at surface and accepted internationally) in time slice experiments.

In the present study, three time-slice experiments are conducted with GME model at 40 km resolution. These experiments are for three different periods i.e. 1979~1983 (considered as Present climate), 2040~2045 (considered as middle climate of 21<sup>st</sup> century) and 2081~2085 (considered as end of 21<sup>st</sup> century climate).

Fig. 5 (a to f) show change in temperatures of three time slice experiments in DJF and JJA seasons. Fig. 5 (a and b) shows mean temperature at 2m during DJF and JJA seasons from 1979 to 1983. Fig. 5 (a and b) clearly shows that Australia and inland area of South America are the warmest regions during DJF while Middle East Asia in JJA. The belts of above 20°C temperature are located near 30S to 30N in DJF and 30S to 40N in JJA. Fig. 5 (c and d) shows the difference between in temperature between middle of 21<sup>st</sup> century and present climate in DJF and JJA respectively. Fig. 5c

## 2m Temperature (°C) by IPCC/SRES A1B

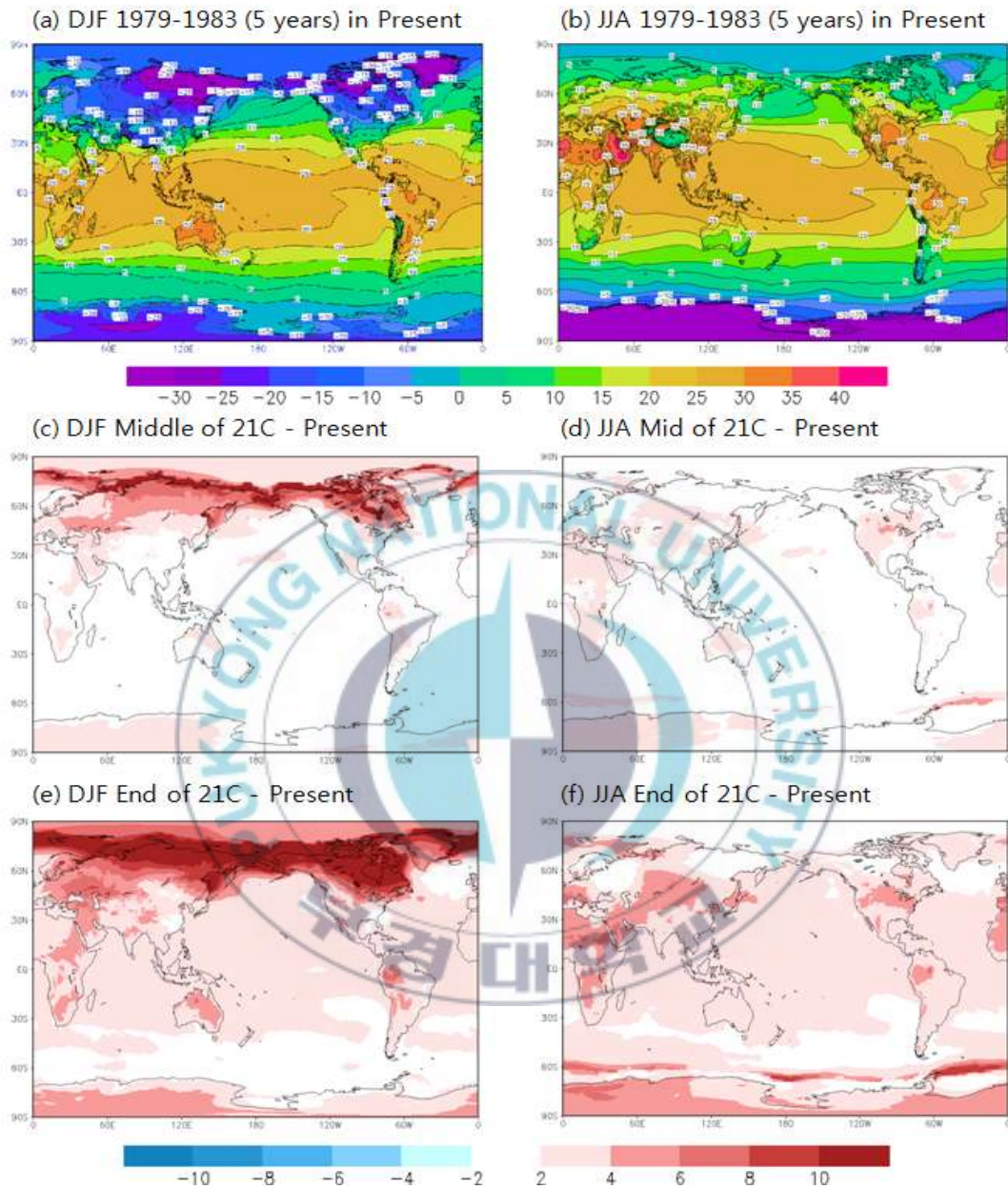


**Fig. 6a-f** (a) Mean temperature of five years at 2m for presents day climate experiment, (b) difference between Middle of 21st century and present experiments and (c) difference between End of 21st century and present experiments in DJF (left panel) and JJA (right panel) seasons.

indicates warming especially over the Arctic region and near the Peru and South America in DJF. While in JJA, Fig. 5d shows small change in temperature than in DJF but a warming signal can easily be seen over the North America and near Brazil in South America. Fig. 5 (e and f) shows the difference in temperature between end of 21<sup>st</sup> century climate and present climate in DJF and JJA seasons respectively. Fig. 5 (e and f) shows strong warming in Antarctic regions and some part of the South America, Australia, Europe and Africa and Arctic region in DJF. In JJA, there is a strong warming signal over the Arctic region and some parts of the America, the Europe, the Africa and the East Asia (fig. 5f).

In addition to temperature change, I have also studied the accompanied difference in the rainfall amount (shown in the Fig. 6) in time slice experiments for the same periods. Fig. 6 exhibits an increasing trend in precipitation, it is an indicative of activated convection. This can be helpful to understand "seeding" of the tropical cyclone generations. These features may be responsible for increasing the frequency of the tropical cyclones over the North Indian Ocean and the North Atlantic Ocean in the Middle of 21<sup>st</sup> century and over the Indian Ocean and Atlantic Ocean in the end of 21<sup>st</sup> century.

### Precipitation (mm) by IPCC/SRES A1B

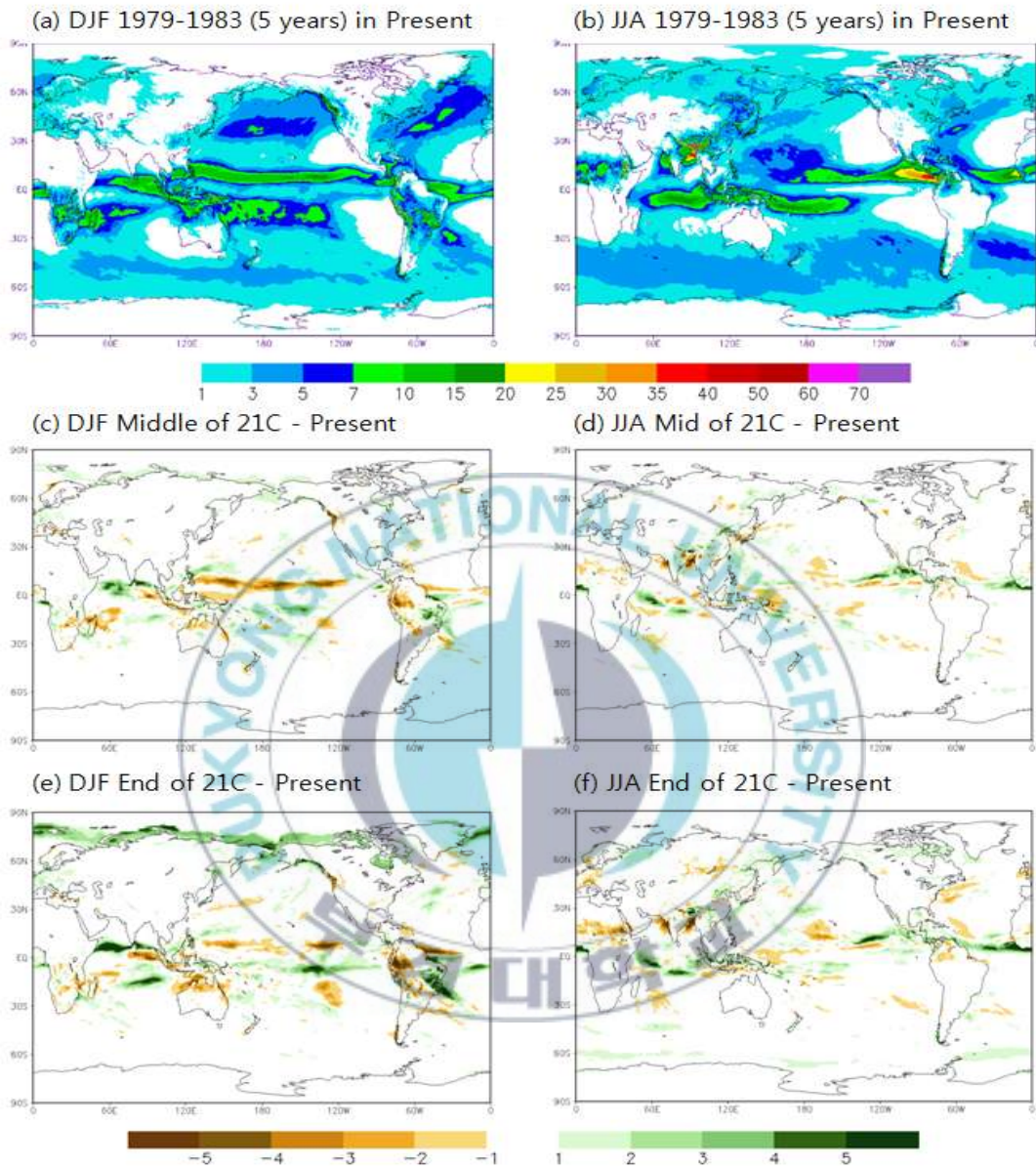


**Fig. 6a-f** Same as in Fig. 5 (a-f) except for precipitation.

## 2. An example of a tropical cyclone

Previous climate models used for tropical cyclone study by different groups using GCM have a coarser mesh compared to GME used in the present study. An advantage of using the 40 km-mesh (high resolution) in GME model, a good improvement in the representation of the inner structures of a tropical cyclone is noticed.

A preliminary five-year integration is completed with the GME model and we are mainly interested to examine the ability of the model in simulating the tropical cyclone. The GME is simulated from January 1979 to December 1983, using the observed SST of the same period. Several realistic tropical cyclone are simulated in this simulation (shown in Fig. 7). Fig. 7 shows lowest central pressure of 968 hPa and maximum wind speed is  $43.7 \text{ m s}^{-1}$  (typhoons simulated with GME).

Figure 8 illustrates horizontal distributions of (a) MSLP (contour) and wind speed at 850 hPa (shaded) over the northwest Pacific region, (b) daily averaged precipitation amount in  $\text{mm hour}^{-1}$  (shaded), (c) relative vorticity (shaded), (d) difference in wind speed between 850 hPa and 300 hPa (shaded), (e) and (f) difference in temperature at 700 hPa and 500 hPa (shaded) and 700 hPa and 300 hPa (shaded) respectively. A comma-shaped high rainfall region, labeled A, spreads immediately outside of the lowest surface pressure region can be seen in Fig. 8(b).

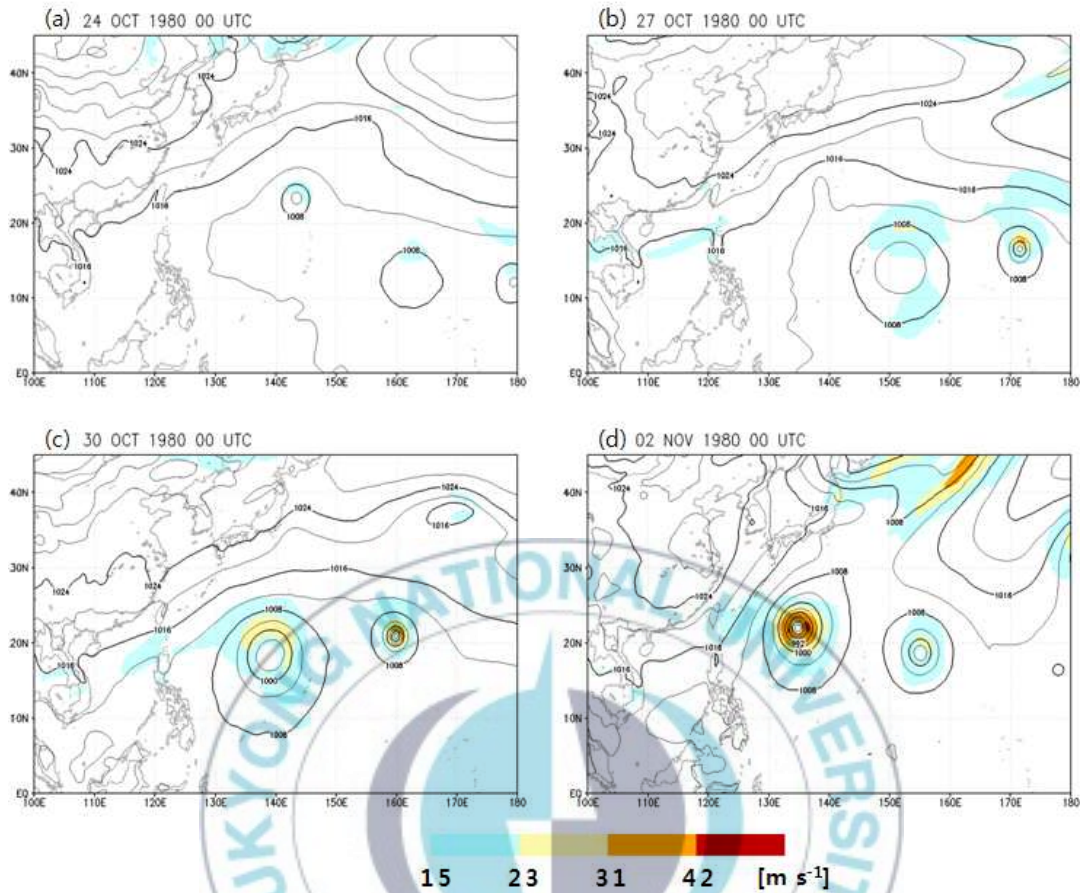


**Fig. 8** A typhoon simulated with the 40 km GME global model. (a) A week tropical storm was generated of the simulation at 14°N, 162°E. (b) The tropical storm moved westward and developed slowly. (c) It developed tropical cyclone over 23 m/s and turned its direction to north-westward. (d) The simulated typhoon wind speed over 42 m/s.

Region A may be likely to be correspond to the eyewall of the tropical cyclone. Figure 8(c-f) indicates that the GME simulation matching well with 6 sets of criteria as mentioned in chapter II. Figure 8c shows

the relative vorticity (shaded) above  $10 \text{ s}^{-1}$  (criteria: exceeding  $3.5 \times 10^{-5} \text{ s}^{-1}$ ) near the center of the tropical cyclone and Figure 8d, shows the difference in wind speed at 850 hPa and 300 hPa and matching well with criteria ie. wind at 850 hPa is larger than wind speed at 300 hPa. In Figure 8d, near the tropical cyclone center, the values are almost positive anomaly. The figure 8e and 8f show the difference in temperature at 700 hPa and 500 hPa, and 700 hPa and 300 hPa respectively. Mos of regions show temperature above 2 K.



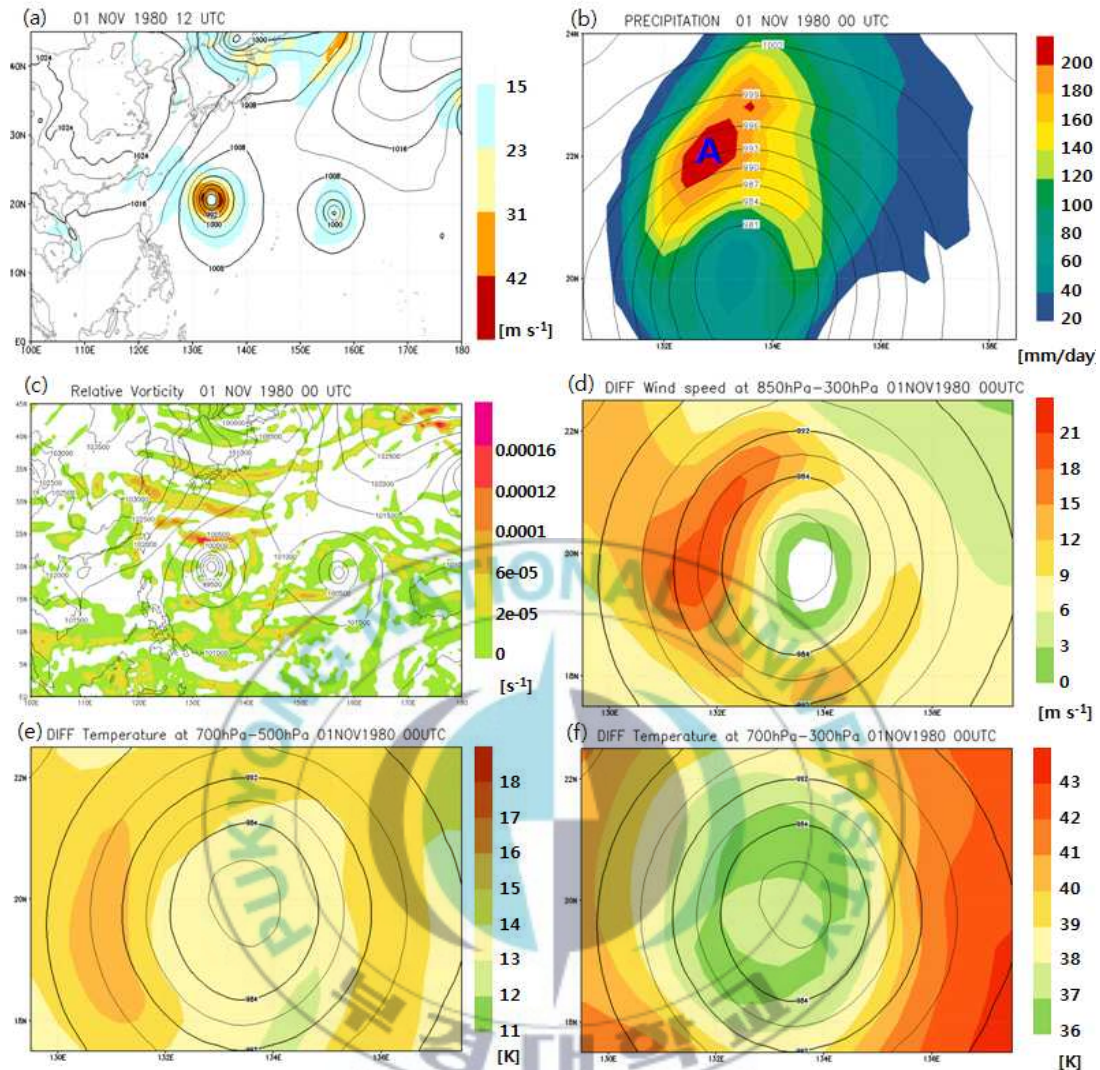


**Fig 9** Horizontal view of a tropical cyclone simulated in the present-day experiment (Nov 1, 2nd year of the time integration): horizontal distributions of (a) PMSL (line) and wind speed at 850 hPa (shaded) in the northwest Pacific region, (b) daily averaged precipitation amount in mm hour<sup>-1</sup> (shaded), (c) relative vorticity (shaded), (d) difference of wind speed at 850 hPa and 300 hPa (shaded), (e)(f) difference of temperature at 700 hPa and 500 hPa (shaded), and 700 hPa and 300 hPa (shaded).

### **3. Tracks and geographical distribution in West Pacific region**

Figure 9 shows the Tropical Cyclone tracks and geographical distribution in West Pacific region. Figure 9 (a) and (b) are observation Tropical Cyclone tracks and present-day simulated Tropical Cyclone tracks in West Pacific region. In figure 9 (b), the initial points of Tropical Cyclones location are more west-ward than figure 9 (a). It may be model bias. Totally, these two figures indicate that the model captured the location and movement of the Tropical Cyclone reasonably well as observation data. Figure 9 (c) and (d) are middle of 21st century and end of 21st century simulated Tropical Cyclone tracks in West Pacific region. Figure 9 (c) and (d) show that the initial point of Tropical Cyclone in middle of 21st century and end of 21st century moves to the northern location than present-day simulation, and in end of 21st century. Figure 9 (b), (c), and (d) also show the reduce of Tropical Cyclone in the future clearly.

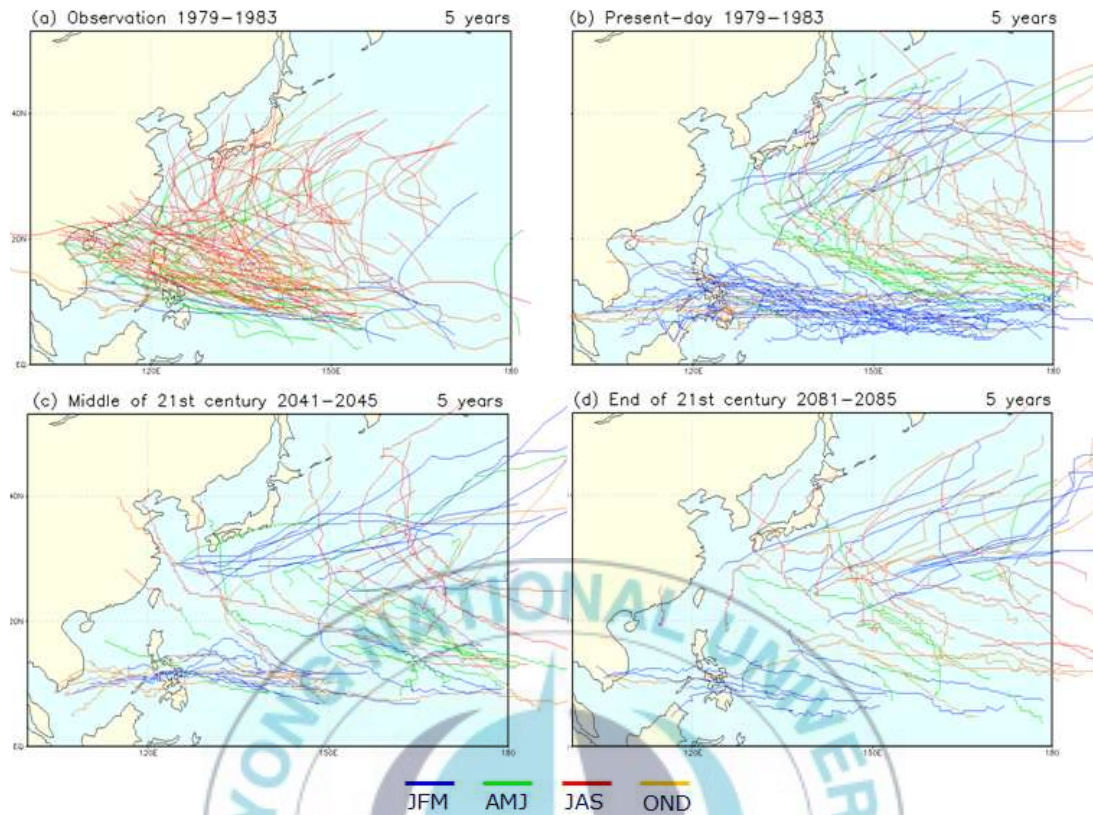


**Fig. 9** Tropical Cyclone tracks in West Pacific region of the observational data (a), the present-day, 1979-1983 (b), the middle of 21st century, 2041-2045 (c), and the end of 21st century, 2081-2085 (d). The tracks detected at different seasons of each year is in different colors (blue for January, February, and March; green for April, May, and June; red for July, August, and September; orange for October, November, and December)

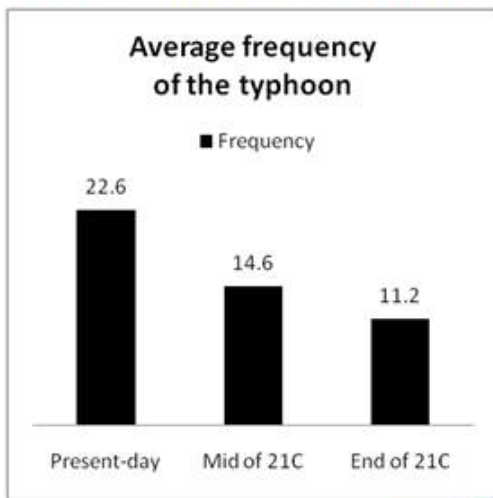
#### **4. Frequency, Duration, and Intensity in West Pacific region**

Figure 10 shows the graphs about frequency, duration and intensity of Tropical Cyclone in West Pacific region. Each black bar indicates the present-day, middle of 21st century, and end of 21st century yearly averaged values during 5-year. In figure 10 (a), frequency of Tropical Cyclone is projected to reduce from present-day to end of 21st century clearly. In present-day, it occurs 22.6 times in a year. It is projected to reduce to 14.6 in middle of 21st century. Difference value between present-day and middle of 21st century is 8. Then it is projected to reduce to 11.2 in end of 21st century. Difference value between present-day and end of 21st century is 11.4. It does not reduce linearly but reduce reasonably well.

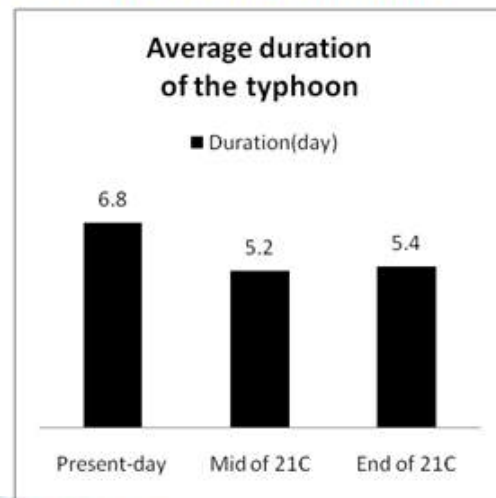
Change of duration of Tropical Cyclone is different than frequency. It also shows the reduction line present-day to middle of 21st century, but it is projected to little increase from middle of 21st century to end of 21st century about 0.2 day. Compare to present-day and future (middle and end of 21st century), it is projected decrease of duration of Tropical Cyclone about 1.5 day.

However, change of intensity of Tropical Cyclone is projected to increase clearly. In present-day, mean value of Tropical Cyclone

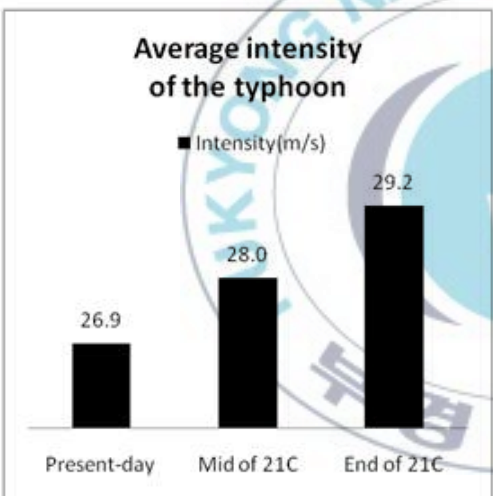
**(a) Yearly average frequency**



**(b) Yearly average duration**



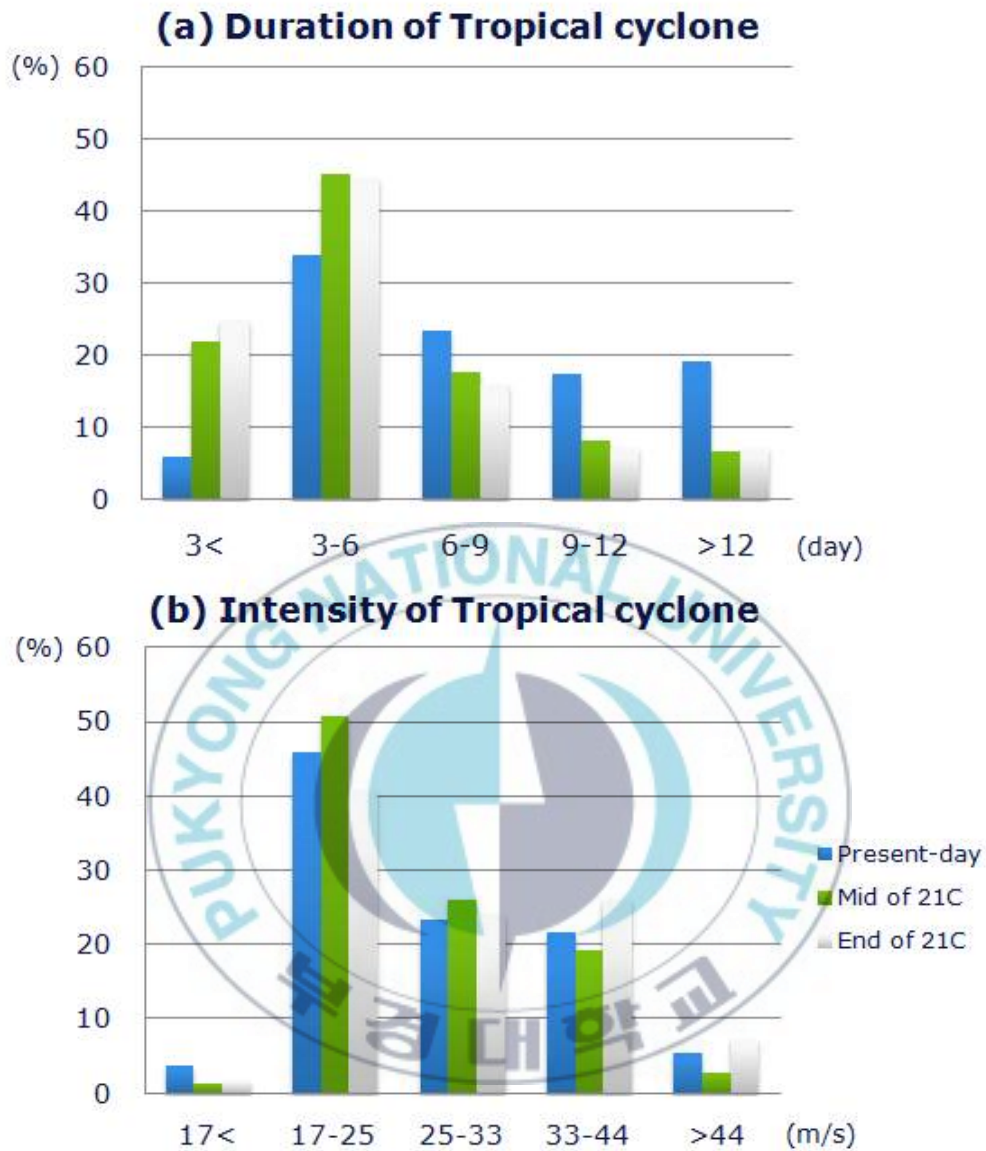
**(c) Yearly average intensity**



**Fig. 11** Each graph shows the change of yearly average frequency (a), yearly average duration (b), and yearly average intensity in present-day, middle of 21 century, and end of 21st century.

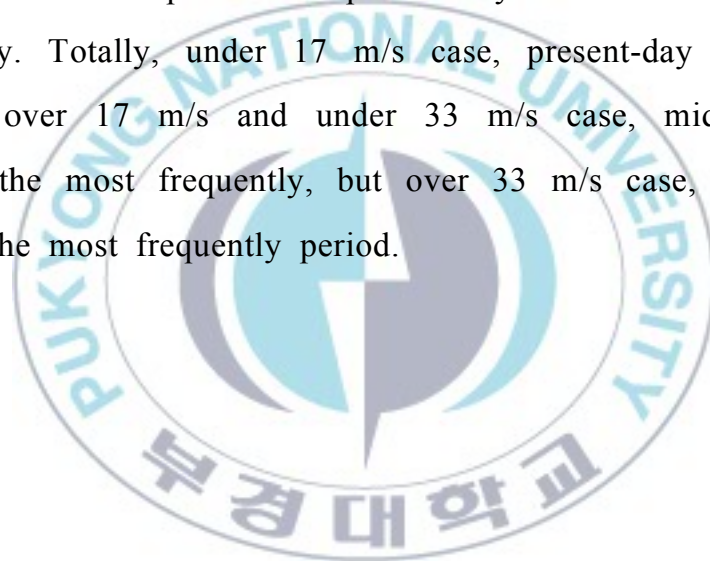
intensity is 26.9 m/s. It is projected to increase about 28.0 m/s in middle of 21st century. Difference value between present-day and middle of 21st century is 1.1 m/s. It means that more strong Tropical Cyclone can be occur in the middle of 21st century. In the end of 21st century, average intensity of Tropical Cyclone is getting stronger than middle of 21st century. It is projected about 29.2 m/s. Difference value between middle of 21st century and end of 21st century is 1.2 m/s. This value is stronger than difference between present-day and middle of 21st century. Compare with present-day and end of 21st century, the difference value is 2.2 m/s. It means that in the future intensity of Tropical Cyclone is getting stronger than present-day. Totally, figure 10 shows the decrease of frequency and increase of intensity in the future clearly.

Figure 11 shows the duration and intensity of Tropical Cyclone. In figure 11 (a), under 3 day case, present-day duration is less than future about 15 more percent, and middle of 21st century is less than end of 21st century about 3%. Over 3 day and under 6 day case present-day is less than future about 12%, but end of 21st century is little less than middle of 21st century. Over 6 day, present-day is more than future. Over 6 day and under 9 day is projected to decrease in the future but over 9 day case middle of 21st century is as same as end of 21st century. Moreover over 12 day case, present-day is more than future about 10%.



**Fig. 12** The duration and intensity of Tropical Cyclone. Blue color shows present-day, green shows the middle of 21st century, and grey shows the end of 21st century.

In figure 11 (b), under 17 m/s case, present-day intensity is more than future Tropical Cyclone intensity, but end of 21st century intensity is stronger than middle of 21st century. Intensity over 17 m/s and under 25 m/s is the most frequently intensity. Intensity of present-day is less than middle of 21st century, but more than end of 21st century. Over 25 m/s and under 33 m/s is as same as over 17 m/s and under 25 m/s but, present-day is less than end of 21st century. Over 33 m/s case, end of 21st century is projected more frequently than other period but present-day is more than middle of 21st century. Totally, under 17 m/s case, present-day is the most frequently, over 17 m/s and under 33 m/s case, middle of 21st century is the most frequently, but over 33 m/s case, end of 21st century is the most frequently period.



## IV. Summary and Conclusion

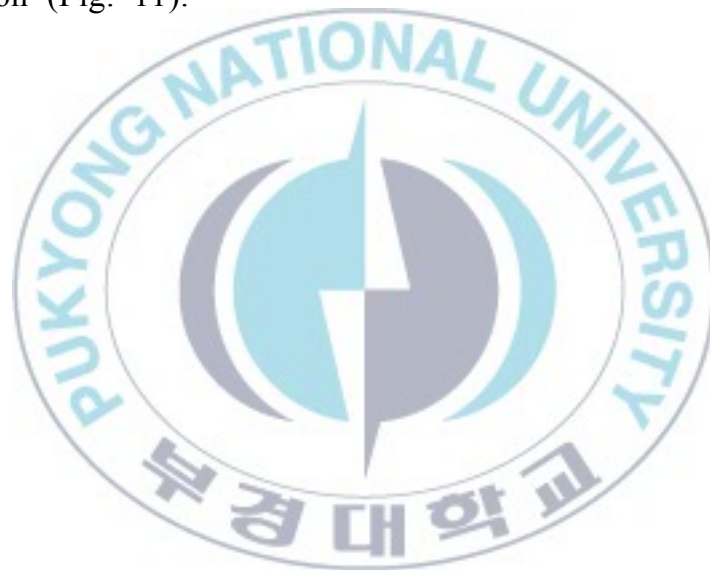
In the present study, performance of high-resolution time-slice experiments corresponding to climate change signal in the latest decades of the twenty-first century under the IPCC A1B emission scenario has been seen using GME model. Present study mainly focuses on the tropical cyclone globally and analysed the tracks and geographical distribution, frequency, duration and intensity of tropical cyclone.

In general, the Control run shows a good performance in reproducing both the mean temperature at 2m (Fig. 5) and precipitation (Fig. 6) patterns along with the underlying large-scale circulation features. It may provide a more reliable projection of the future tropical cyclone.

The present study clearly indicates that for a reliable prediction of future climatology of tropical cyclone under different climate change scenarios, it requires not only a realistic simulation of tropical cyclones with a high-resolution models, but also a reliable estimate of SST and Sea-Ice change with a low resolution coupled GCMs is highly needed.

Under the SRES A1B scenario, the results of GME time-slice

simulation are the frequency is projected to decrease, the duration is projected to decrease and the intensity is projected to increase over the West Pacific region (Fig. 10). Further more, in future, long Tropical Cyclone duration is projected to decrease, and short Tropical Cyclone duration is projected to increase. Week intensity Tropical Cyclones are projected decrease, and strong Tropical Cyclones are projected increase in middle of 21st century and severe Tropical Cyclones are projected increase in end of 21st century in West Pacific region (Fig. 11).



## Reference

- Bengtsson, L., K.I. Hodges, M. Esch, N. Keenlyside, L. Kornbluh, J.-J. Luo, and T. Yamagata. 2007. How may tropical cyclones change in a warmer climate? *Tellus*, **59A**, 539-561.
- Bengtsson, L., M. Botzet, and M. Esch, 1996: Will greenhouse gas-induced warming over the next 50 years lead to higher frequency and greater intensity of hurricanes? *Tellus*, **48A**, 57-73.
- Doms, G. and U. Schättler, 2003: The nonhydrostatic limited-area model LM (Lokal-Modell) of DWD. *Part I: Scientific Documentation*.
- Hasegawa, A. and S. Emori, 2005: Tropical Cyclones and Associated Precipitation over the Western North Pacific: T106 Atmospheric GCM Simulation for Present-day and Doubled CO<sub>2</sub> Climates. *SOLA*, **1**, 145-148.
- Heise, E. and R. Schrodin, 2002: Aspects of snow and soil modelling in the operational short range weather prediction models of the German Weather Service. *Journal of Computational Technologies, Special Issue: Proceedings of the International Conference on Modelling, Databases and Information Systems for Atmospheric Science (MODAS)*, **7**, 121-140.
- IPCC, 2007: *Climate Change 2007: The Physical Science Basis. Contribution of Working Group I to the Fourth Assessment Report of the Intergovernmental Panel on Climate Change*. Cambridge University Press, Cambridge, United Kingdom and New York, NY, USA, 996pp.
- IPCC, 2001: *Climate change 2001: The Scientific Bases. Contribution of Working Group I to the Third Assessment Report of the*

*Intergovernmental Panel on Climate Change*. Cambridge University Press, United Kingdom and New York, NY, USA, 881pp.

Knutson, T.R. et al. 2001: Impact of CO<sub>2</sub>-Induced Warming on Hurricane Intensities as Simulated in a Hurricane Model with Ocean Coupling, *Journal of Climate*, **13**, 109-121.

Knutson, T.R., R. E. Tuleya, and Y. Kurihara, 1998: Simulated increase of hurricane intensities in a CO<sub>2</sub>-warmed climate. *Science*, 279, 1018-1020.

Lott, F., and M. Miller, 1997: A new sub-grid scale orographic drag parameterization: Its formulation and testing, *Quart. J. Roy. Meteor. Soc.*, **123**, 101-128.

Louis, J. -F., 1979: A parametric model of vertical eddy fluxes in the atmosphere, *Bound.-Layer Meteor.*, **17**, 187-202.

Majewski, D. and Coauthors, 2002: The Operational Global Icosahedral-Hexagonal Gridpoint Model GME: Description and High-Resolution Tests. *Mon. Wea. Rev.*, **130**, 319-338

Majewski, D., D. Liermann, P. Prohl, B. Ritter, M. Buchhold, T. Hanisch, G. Paul, W. Wergen and J. Baumgardner, 2000: The global icosahedral-hexagonal grid point model GME -Operational version and high resolution tests-, *ECMWF Workshop Proceedings*, Numerical methods for high resolution global models.

Majewski, D. 1998: The new global icosahedral-hexagonal grid point model GME of the Deutscher Wetterdienst, *Proc. ECMWF*

*Seminar on Recent Developments in Numerical methods for Atmospheric Modelling*, ECMWF, Reading, United Kingdom, 173-201.

Mellor, G. L., and T. Yamada, 1974: A hierarchy of turbulence closure models for planetary boundary layers, *J. Atmos. Sci.*, **31**, 1791-1806.

Müller, E., 1981: Turbulent flux parameterization in a regional-scale model, *Proc. ECMWF Workshop on Planetary Boundary Layer Parameterization*, ECMWF, Reading, United Kingdom, 193-220.

Oouchi, K. et al., 2006: Tropical Cyclone Climatology in a Global-Warming Climate as Simulated in a 20 km-Mesh Global Atmospheric Model: Frequency and Wind Intensity Analyses, *Journal of the Meteorological Society of Japan*, **84**, 259-276

Ringler, T. D., R. P. Heikes, and D. A. Randall, 2000: Modeling the atmospheric general circulation using a spherical geodesic grid: A new class of dynamic cores. *Mon. Wea. Rev.*, **128**, 2471-2490.

Ritter, B., and J.-F. Geleyn, 1992: A comprehensive radiation scheme for numerical weather prediction models with potential applications in climate simulations, *Mon. Wea. Rev.*, **120**, 303-325.

Simmons, A. J., and D. M. Burridge, 1981: An energy and angular-

- momentum conserving vertical finite-difference scheme and hybrid vertical coordinate. *Mon. Wea. Rev.*, **109**, 758-766.
- Sugi, M. et al., 2002: Influence of the global warming on tropical cyclone climatology: An experiment with the JMA global model. *J. Meteor. Soc. Japan*, **80**, 249-272
- Tiedtke, M., 1989: A comprehensive mass flux scheme for cumulus parameterization in large-scale models, *Mon. Wea. Rev.*, **117**, 1779-1800.
- Tomita, H. and Satoh, M., 2004 : A new dynamical framework of nonhydrostatic global model using the icosahedral grid. *Fluid Dyn. Res.*, **34**, 357-400.
- Tsutsui, J-I., 2002: Implications of anthropogenic climate change for tropical cyclone activity: A case study with the NCAR CCM2. *J. Meteor. Soc. Japan*, **80**, 45-65.
- Webster et al., 2005: Changes in Tropical cyclone Number, Duration, and Intensity in a Warming Environment, *Science*, **309**, 1844-1846.
- Yoshimura, J., M. Sugi, and A. Noda, 2006. Influence of greenhouse warming on tropical cyclone frequency, *Journal of the Meteorological Society of Japan*, **84**, 405-428.
- Yoshimura, J. and M. Sugi, 2005: Tropical cyclone climatology in a high-resolution AGCM – Impacts of SST warming and CO<sub>2</sub> increase. *Sci. Online Lett. Atmos.*, **1**, 133 - 136.